

[20002]

## 照射誘起アモルファス化への Fe イオンビーム影響

### Effect of iron beam on radiation-induced amorphization

叶野翔<sup>A)</sup>, 楊会龍<sup>A)</sup>, 安堂正己<sup>B)</sup>, 阿部弘亨<sup>A)</sup>

Sho Kano<sup>A)</sup>, Huilong Yang<sup>A)</sup>, Masami Ando<sup>B)</sup>, Hiroaki Abe<sup>A)</sup>

<sup>A)</sup> Nuclear Professional School, School of Engineering, The University of Tokyo

<sup>B)</sup> National Institutes for Quantum and Radiological Science and Technology (QST),  
Research and Development Center

#### Abstract

The purpose of the present study is to clarify the instability behavior of  $M_{23}C_6$  under irradiation, specifically the occurrence of radiation-induced amorphization. Ion irradiation of 10.5 MeV- $Fe^{3+}$  at elevated temperatures from 573-623 K was conducted into the reduced activation ferritic/martensitic steels (F82H). A bilayer contrast of the particle consisting of an amorphous-rim phase and inner crystalline core of  $M_{23}C_6$  was observed after irradiation. From the high-resolution electron microscope observation, the preferential occupation site of W into  $M_{23}C_6$  lattice was identified as 8c-site prior to irradiation in F82H specimen, which shifted to other sites due to chemical disordering due to irradiation. Evaluation of the intensity ratio between 8c and another site of  $M_{23}C_6$ , 8c/4a, then revealed that the extent of chemical disordering of W was mitigated at the amorphous-crystal interface region in comparison with the central of the particle.

**Keyword:** radiation-induced amorphization, chemical disordering,  $M_{23}C_6$ , HAADF, F82H,

#### 1. Introduction

F82H (Fe-8Cr-2W, V, Ta) steel is one of the candidate structural materials for fusion reactors. Research and development of F82H steel for optimizing the material design and fabrication procedure for the fusion DEMO-blanket system has been conducted for 30 years. Various basic mechanical properties of F82H have been reported in numerous papers so far. Properties such as weldability<sup>[1]</sup>, irradiation tolerance<sup>[2]</sup>, and thermal fatigue<sup>[3]</sup> are important for the application of fusion reactor have been evaluated with 14 MeV-neutron irradiation under elevated temperatures (573-823 K). The nano-scale fine particles such as MX (M: Ta and V, X: C and N) and  $M_{23}C_6$  (M: Cr, Fe, and W) are co-precipitated in this material<sup>[4]</sup>. In particular, the irradiation resistance and thermal stability of these particles are very important factors to maintain their excellent mechanical property at severe high temperature and irradiation environments.

The investigations into the tensile behaviors of F82H steel after irradiation have been widely conducted<sup>[5]</sup>, although the necessary engineering data for fusion reactor design such as creep and fatigue under irradiation is still lacking. Thus, the prediction of the creep properties during and after irradiation is currently recognized as an important challenge, which necessitates the precise understanding of microstructural evolution accompanying high temperature and irradiation accumulation. Regarding the creep properties of F82H<sup>[6]</sup>,  $M_{23}C_6$  has inhibited the grain boundary migration, and it's contributing maintain the integrity of the initial microstructural features. Meanwhile, the laves phase formed by the long-term thermal aging is detrimental to the creep property, resulting in significant degradation of the material<sup>[7]</sup>.

Predicting this behavior under the fusion reactor operation is thus greatly important because the formation of the laves may be accelerated by the radiation-enhanced diffusion.

Several efforts have been made to investigate the stability of these particles under irradiation, e.g., the crystal to amorphous transformation known as the radiation-induced amorphization (RIA) was reported in  $M_{23}C_6$  under neutron irradiation at 573 K even at a relatively lower dose condition<sup>[8]</sup>. Although this formation behavior has not been well understood, this result suggests that the competing reaction between the amorphization of  $M_{23}C_6$  and the formation of the laves phase has to be considered under the reactor environment. In our previous studies<sup>[9-11]</sup>, the RIA of  $M_{23}C_6$  under ion-accelerator irradiations with various temperatures and dose conditions was conducted to clarify the feature of amorphization of  $M_{23}C_6$ . As a result, the critical dose to amorphization was estimated as  $\sim 1.0$  dpa (displacement per atom) under the 2.8 MeV- $Fe^{n+}$  at room temperature (RT) irradiation, and this critical dose increases with an increase in irradiation temperature. Besides, the amorphization of the particle could be observed in the irradiation temperature below 623 K. Despite the fact that various RIA behaviors have been experimentally confirmed, elucidation of the RIA mechanism still remains an open question, which is necessary in order to predict the instability behavior of  $M_{23}C_6$  under a fusion reactor environment.

Research interest about the solid to solid amorphization (SSA) under irradiation has been intensely investigated for a long time in the irradiation materials community, among them RIA has been reported to occur mainly in the intermetallic compounds and oxides (ceramics)<sup>[12]</sup>. So far, several possible mechanisms have been proposed to

[20002]

explain the RIA phenomena, such as the accumulation of irradiation defect including the anti-site defect formation<sup>[13]</sup>, chemical disordering<sup>[14]</sup>, chemical composition change<sup>[15]</sup>, phase transformation involving the precipitation of secondary phase<sup>[16]</sup> and so on. The basic idea behind these mechanisms is that the amorphous phase would be formed when the crystallographic changes accompanying irradiation exceeds the amorphous energy state. In addition, the correlation between the SSA by irradiation and the metallurgical rapid cooling amorphization (RCA) has been investigated. It is noteworthy to mention here that, the amorphous phase was confirmed followed by the SSA process but not in the RCA process in some of the systems<sup>[17]</sup>, and that the atomic arrangement of short-range ordering in the SSA amorphous does not correspond to the feature of RCA-phases.

The purpose of the present study is to clarify the RIA mechanism of  $M_{23}C_6$  in F82H steel under the cascade damage condition. Ion accelerator irradiation was utilized in this study to introduce cascade damage into the material, it will help us to do this research because the irradiation parameters such as the irradiation dose and temperature condition can be accurately controlled. Although the main elements of  $M_{23}C_6$  in F82H steel are Fe, Cr, and C, but a small amount of W, V, and Ta atoms are also contained. Thus, the effect of minor elements of  $M_{23}C_6$  especially W on the RIA behavior was systematically investigated in this study using in both conventional selected area electron diffraction and high-resolution electron microscopy observation.

## 2. Experimental procedures

The chemical compositions of F82H specimen is The chemical compositions of F82H is Fe-0.1C-7.88Cr-1.78W-0.19V-0.09Ta-0.45Mn-0.022Al-0.001O-0.001N. F82H was fabricated by elected arc melting with electron slag re-melting processes. The heat treatment condition of normalizing and tempering was 1313 K for 2.4 ks and 1023 K for 3.6 ks, respectively. Detailed information on the thermal history of this specimen can be seen elsewhere<sup>[10]</sup>.

Specimens with a size of  $1 \times 3 \times 5 \text{ mm}^3$  were prepared for the ion irradiation. They were firstly cut from the bulk specimen, and subsequently grinded with emery papers of P400-2000. The surface was further mirror-finished by polishing with alumina slurry ( $0.25 \mu\text{m}$ ) and colloidal silica suspensions ( $50 \text{ nm}$ ). Finally, the deformed layer induced by mechanical polishing was removed by electrochemically etching in a solution (8% - perchloric acid in acetic acid) at 298 K at the voltage of 24 V, the current of 0.1 A, and the polishing time of 15 s.

The ion irradiation using  $10.5 \text{ MeV-Fe}^{3+}$  as the ion beam was conducted at 573, 598, and 623 K at the TIARA facility, National Institutes for Quantum and Radiological Science and Technology. The irradiation temperature was

monitored and recorded by a radiation thermometer. The depth profile of irradiation damage was evaluated with SRIM calculation code<sup>[18]</sup>. The damage rate is determined based on the average Fe-beam flux and the SRIM displacement calculation with the Kinchin-Pease model. The threshold displacement energy for Fe ( $E_{d,Fe}$ ) was set as 40 eV in this calculation<sup>[19]</sup>. The depth at the damage peak is  $\sim 2.1 \mu\text{m}$  away from the surface, with the corresponding irradiation rate of  $3.7 \times 10^{-3} \text{ dpa/s}$ . It is also noted that the local irradiation dose at a specific region for TEM examination was estimated individually based on the depth from the surface for each irradiated specimen, to record a precise irradiation history. In this study, the irradiation damage of each specimen was designated as the dose at the depth of  $1.0 \mu\text{m}$  away from the surface, which is 20 dpa.

After irradiation, cross-sectional transmission electron microscopy (TEM) observation was conducted to investigate microstructural changes due to irradiation. A standard lift-out method using the focused ion beam (FIB) technique was applied to prepare the thin TEM specimens in a Hitachi FB-2100 system. The acceleration voltage of Ga ions was set to 40 kV, and a W-deposit layer was applied to protect the thin foil from the irradiation damage induced by Ga-ion during FIB process. Then, the two step low energy Ar ion milling which is 1.0 and 0.3 kV in working voltage was performed before TEM observation to eliminate the artificial defects induced by FIB processing.

TEM observation and scanning transmission electron microscopy-energy dispersive X-ray spectrometry (STEM-EDS) were conducted on JEOL JEM-2100 and FEI Titan3 G2 microscopes (Titan3), Titan3 is a probe spherical aberration-corrected (Cs-corrected) microscope was utilized for the atomic-scale observation, the image resolution, probe size, and convergence semi-angle of electron probe, were 70 pm,  $<0.1 \text{ nm}$ , and 17.9 mrad, respectively. The working voltage for JEM-2100 and Titan3 were respectively 200- and 300-keV. Bright field (BF), dark field (DF), and annular dark field (ADF) observations with the selective area electron diffraction (SAED) analysis were utilized to evaluate the morphological change of the particles.

The simulation of the ADF images was conducted in MacTempas software. The space group of  $M_{23}C_6$  is  $Fm\bar{3}m$ , in which 116 atoms exist in an unit cell<sup>[20]</sup>. Previous studies pointed out that carbon atoms would occupy 24e sites with coordinate of (0.277, 0, 0), and the metric atoms such as Cr, Fe, and W, are located at the four Wyckoff sites, namely 4a, 8c, 32f, and 48h. The coordinate is respectively (0, 0, 0), (0.25, 0.25, 0.25), (0.381, 0.381, 0.381), and (0, 0.170, 0.170) for 4a, 8c, 32f, and 48h site. In the present simulation, the convergence semi-angle of the electron probe and the ADF collector angles are set as 17.9 mrad and 30-90 mrad, and Scherzer focus, spherical aberration, chromatic aberration coefficient, and thermal

[20002]

diffuse scattering runs are set as 0. The values applied here are not exactly the same with the experimental ADF imaging parameters, the experiment ADF image cannot be completely represented by the MacTempas simulation. However, it is believed that the features such as atomic arrangement and intensity ratio of each atomic column in  $M_{23}C_6$  can be represented by the experimental observation. Therefore, in order to determine the lattice site of W in  $M_{23}C_6$ , the dependency of intensity variation on the substitution atom in  $M_{23}C_6$  was evaluated by MacTempas simulation, it was then compared to the atomic-scale micrograph in this study.

### 3. Results and Discussions

Fig. 1 shows the morphology of particles irradiated at 573, 598, and 623 K with an irradiation dose of 20 dpa in F82H specimens. BF, DF, and the corresponding SAED with indexing of both Fe and  $M_{23}C_6$  phases were summarized in this figure. The incidence electron beam direction (Z-direction) of  $M_{23}C_6$  irradiated at 573, and 598 and 623 K are  $[\bar{1}22]$ , and  $[011]$  respectively. From the BF image, a bilayer contrasted  $M_{23}C_6$  can be clearly observed in all the specimens. In addition, SAED analyses showed the appearance of both diffraction spot and halo ring in specimens of 573 and 598 K, in which the interplanar spacing of the halo-ring is calculated to be approximately consistent with (333) of  $M_{23}C_6$ . DF observation exposed from the halo-ring showed its consistency with an outside layer surrounding the core, revealing the amorphization at the out-layer and leaving still crystalline at the core-layer in  $M_{23}C_6$ . Despite that no clear halo-ring was observed from the SAED in the specimen of 623 K, the DF-image taken from  $g=\bar{4}2\bar{2}$  showed an obvious low contrast layer on the surrounding of  $M_{23}C_6$  particle. The d-spacing of ( $\bar{4}2\bar{2}$ ) reflection was close in value to the (333) halo-ring, indicating that a similar RIA phenomenon occurred in this specimen. In addition, the absence of the halo-ring at 623 K suggests that the RIA in  $M_{23}C_6$  particle might be weakened or delayed by an increase in temperature. To summarize, the RIA of  $M_{23}C_6$  in F82H steel under irradiation at  $<623$  K shows a bilayer contrast, consisting of an amorphous-rim phase and inner crystalline core, to be specific.

High resolution electron microscopy (HREM) micrographs of un-irradiated and irradiated  $M_{23}C_6$  in F82H specimen are summarized in Fig. 2. The irradiation temperature and dose condition are respectively 623 K and 20 dpa. The Z-direction was parallel to the zone axis of  $[011]$  of  $M_{23}C_6$  in both specimens. The long-range periodic sequence of atoms was observed in both specimens although the brightness of each column is clearly different before and after irradiation, and no-structural change between the center and interface region was confirmed. Furthermore, extra structures such as the re-precipitation of secondary phases was not identified at the interface between the crystal and amorphous regions.

The intensity of each atomic column was obviously different from the un-irradiated and irradiated  $M_{23}C_6$  particles, the line profile plotted along three atomic columns was thus evaluated. The result is indicated in Fig. 1(b). The greatest intensity was shown at site 4a as indicated from the directions of (i)- and (ii), no matter if the particle was irradiated or not, and the change in intensity ratio between 4a- and 48h-site was also not observed. On the other hand, the intensity of the 8c-site which is the preferential substitution site of W was similar to the 4a-site in the un-irradiated F82H specimen as shown in the (iii)-direction. However, it was significantly decreased in the irradiated specimen, and this tendency could be confirmed as well at the interface regions. Different intensity behaviours at the 8c-site observed before and after irradiation indicate that W atoms were relocated to the lattice sites of 4a-, 8c-, 32f- and 48h-site when being irradiated, since 8c-site is occupied by W atom. In other words, it is clarified from this HREM analysis that the chemical disordering of W in  $M_{23}C_6$  lattice would steadily occur upon irradiation.

Wang et. al. reported that the amorphous domain in size of 2-3 nm was observed in the compound of  $Ca_2La_8(SiO_4)_6O_2$  under 1.5 MeV-Kr<sup>+</sup> irradiation at 300 K with in-situ observation<sup>[21]</sup>. The formation of the amorphous domain was explained by a large amount of irradiation defects that survived in the cooling process after the collision cascade event, and the concentration of irradiation defects reached the critical level locally. However, the amorphous domain feature was not observed in our study. It suggests that most of the atoms returned back to the lattice positions during the cooling process after the collision cascade in  $M_{23}C_6$ . This discrepancy with Wang's study might be attributed to a fewer number of point defects formed in  $M_{23}C_6$  in comparison with the complicated oxide system. More types of point defects, such as vacancies, interstitials, and anti-site defects in each sub-lattice, are reported in complex oxide materials, as well as the variable states of these defects because they can react with each other. On the other hand, although the feature of point defect in  $M_{23}C_6$  is still unclear, the defects formed under the present irradiation are presumed to follow simple rules. Such an assumption could provide a rational explanation for the absence of a local amorphous domain in  $M_{23}C_6$  particle in this study.

[20002]

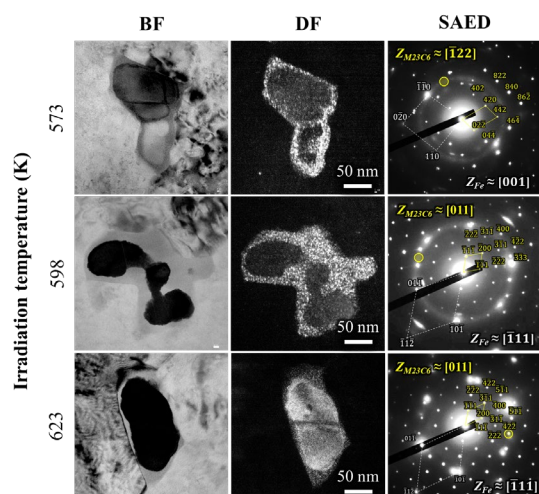


Figure 1. Morphology of particles irradiated at 573, 598, and 623 K with irradiation dose of 20 dpa in F82H specimens. BF, DF, and the corresponding SAED with indexing of both Fe and  $M_{23}C_6$  phases are shown. The Z-direction of  $M_{23}C_6$  irradiated at 573, and 598, 623 K are  $[\bar{1}22]$ , and  $[011]$  respectively, DF images were exposed from halo-ring or  $g=\bar{4}2\bar{2}$  of  $M_{23}C_6$  that as indicated with the yellow circle in SAED.

#### 4. Conclusions

The RIA behaviors of  $M_{23}C_6$  particle in F82H steel was systematically investigated by ion accelerator irradiations at temperatures ranging from 573 to 623 K. After irradiation, detailed TEM observations using both the conventional STEM analysis, atomic structure characterization, and chemical composition analyses were conducted to clarify the underlying mechanism of the chemical substitution dependent RIA. The main results of this study are summarized as follows:

- (1) The RIA behavior of  $M_{23}C_6$  was confirmed in the irradiated F82H specimen, the feature of RIA-particle was a bilayer structured consisting of crystalline core and amorphous shell was observed, indicating that RIA preferentially occurred at the interface between the particle and matrix.
- (2) Based on the combined HREM observation and atomic structure simulation, it is revealed that the preferential location site of W in  $M_{23}C_6$  is 8c site. When the 8c site is fully filled by W atoms, the concentration of W was theoretically 6.9 at.%, which is fairly close to the experimental result.
- (3) The chemical disordering of W into the irradiated  $M_{23}C_6$  was observed, but the intensity ratio between 8c and another site of particle, which is an index of the magnitude of chemical disordering, revealed that the chemical disordering was mitigated at the amorphous-crystal interface region in comparison with the center of the particle.

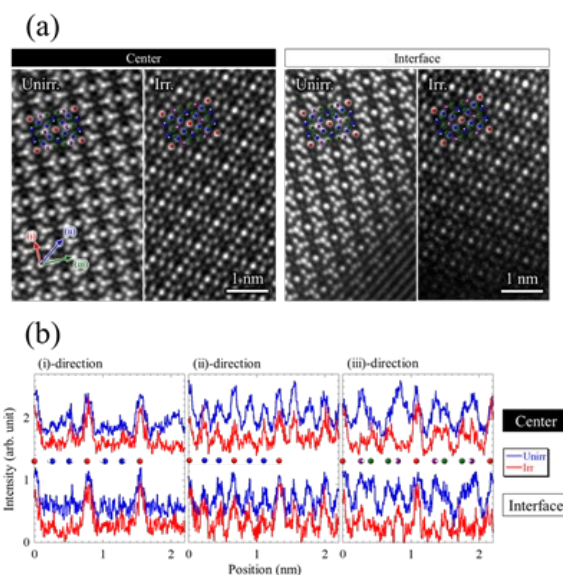


Figure 2. (a) HREM images of un-irradiated and irradiated  $M_{23}C_6$  particles in F82H specimen and (b) line profile results of contrast intensities along (i)-, (ii)-, and (iii)-direction of  $M_{23}C_6$ . The irradiated condition is 623 K and 20 dpa. The Z-direction was parallel to the zone axis of  $[011]$  of  $M_{23}C_6$  for both un-irradiated and irradiated specimens. The collection semi-angle of HAADF image was set as 126-200 mrad. The white, green, blue, red, and purple atoms are respectively indicated as 24e, 32f, 48h, 4a, 8c site in a  $M_{23}C_6$  lattice.

#### References

- [1] T Sawai, K Shiba, A Hishinuma, Microstructure of welded and thermal-aged low activation steel F82H IEA heat, J. Nucl. Mater., 283-287 (2000) 657-661.
- [2] K. Shiba, M. Suzuki, A. Hishinuma, Irradiation response on mechanical properties of neutron irradiated F82H, J. Nucl. Mater., 233-237 (1996) 309-312.
- [3] J.F. Stubbins, D.S. Gelles, Fatigue performance and cyclic softening of F82H, a ferritic-martensitic steel, J. Nucl. Mater., 233-237 (1996) 331-335.
- [4] S. Kano, H.L. Yang, R. Suzue, Y. Matsukawa, Y. Satoh, H. Sakasegawa, H. Tanigawa, H. Abe, Precipitation of carbides in F82H steels and its impact on mechanical strength, Nucl. Mater. & Energy, 9 (2016) 331-337.
- [5] K. Shiba, A. Hishinuma, Low-temperature irradiation effects on tensile and Charpy properties of low-activation ferritic steels, J. Nucl. Mater., 283-287 (2000) 474-477.
- [6] L. Tan, Y. Katoh, A.A.F. Tavassoli, J. Henry, M. Rieth, H. Sakasegawa, H. Tanigawa, Q. Huang, Recent status and improvement of reduced-activation ferritic-martensitic steels for high-temperature service, J. Nucl. Mater., 479 (2016) 515-523.
- [7] R.L. Klueh, Reduced-activation steels: Future development for improved creep strength, J. Nucl. Mater., 378 (2008) 159-166.
- [8] H. Tanigawa, H. Sakasegawa, H. Ogiwara, H. Kishimoto, A. Kohyama, Radiation induced phase instability of precipitates in reduced-activation ferritic/martensitic steels,

[20002]

- J. Nucl. Mater., 367-370 (2007) 132-136.
- [9] S. Kano, H.L. Yang, J. McGrady, D. Hamaguchi, M. Ando, H. Tanigawa, H. Abe, Study of radiation-induced amorphization of  $M_{23}C_6$  in RAFM steels under iron irradiations, J. Nucl. Mater., 533 (2020) 152088 (pp. 10).
- [10] S. Kano, H. Yang, J. Shen, Z. Zhao, M. John, D. Hamaguchi, M. Ando, H. Tanigawa, H. Abe, Investigation of instability of  $M_{23}C_6$  particles in F82H steel under electron and ion irradiation conditions, J. Nucl. Mater., 502 (2018) 263-269.
- [11] S. Kano, H.L. Yang, J.J. Shen, Z. Zhao, J. McGrady, D. Hamaguchi, M. Ando, H. Tanigawa, H. Abe, Instability of MX and  $M_{23}C_6$  type precipitates in F82H steels under 2.8 MeV  $Fe^{2+}$  irradiation at 673 K, Nucl. Mater. & Energy, 17 (2018) 56-61.
- [12] R.W. Cahn, W.L. Johnson, Review: The nucleation of disorder, J. Mater. Res., 1 (1986) 724-732.
- [13] H. Inui, H. Mori, H. Fujit, Electron-irradiation-induced crystalline to amorphous transition in  $\alpha$ -SiC single crystals, Phil Mag. B, 61 (1990) 107-124.
- [14] H. Inui, H. Mori, A. Suzuki, H. Fujita, Electron-irradiation-induced crystalline-to-amorphous transition in  $\beta$ -SiC single crystals, Phil. Mag. B, 65 (1992) 1-14.
- [15] A.T. Motta, C. Lemaignan, A ballistic mixing model for the amorphization of precipitates in Zircaloy under neutron irradiation, J. Nucl. Mater., 195 (1992) 277-285.
- [16] J.N. Mitchell, N. Yu, K.E. Sickafus, M.A. Nastasi, K.J. McClellan, Ion irradiation damage in geikielite ( $MgTiO_3$ ), Phil Mag. A 78 (1998) 713-725.
- [17] T. Nagase, A. Nino, T. Hosokawa, Y. Umakoshi, Electron Irradiation Induced Crystal-to-Amorphous-to-Crystal Transition in Some Metallic Glasses, Mater. Trans., 48 (2007) 1651-1658.
- [18] J.F. Ziegler, J.M. Manoyan, The stopping of ions in compounds, Nucl. Inst. & Methods, B, 35 (1988) 215-228.
- [19] A.Y. Konobeyev, U. Fischer, Y.A. Korovin, S.P. Simakov, Evaluation of effective threshold displacement energies and other data required for the calculation of advanced atomic displacement cross-sections, Nucl. Energy Tech., 3 (2017) 169-175.
- [20] A. Westgren, Complex Chromium and Iron Carbides, Nat., 132 (1933) 430.
- [21] L.M. Wang, W. J. Weber, Transmission electron microscopy study of ion-beam induced amorphization of  $Ca_2La_8(SiO_4)_6O_2$ , Phil. Mag., 79 (1999) 237-253.